Journal of
Materials Chemistry C

ROYAL SOCIETY OF CHEMISTRY

COMMUNICATION

View Article Online
View Journal | View Issue

Cite this: *J. Mater. Chem. C*, 2014, **2**, 7176

Received 21st May 2014
Accepted 17th July 2014

DOI: 10.1039/c4tc01054j

www.rsc.org/MaterialsC

Thickness dependence of the piezoresistive effect in p-type single crystalline 3C-SiC nanothin films†

Hoang-Phuong Phan,*[a] Dzung Viet Dao,[ab] Philip Tanner,[a] Jisheng Han,[a] Nam-Trung Nguyen,[a] Sima Dimitrijev,[ab] Glenn Walker,[a] Li Wang[a] and Yong Zhu[ab]

Published on 18 July 2014. Downloaded by Griffith University on 3/14/2021 10:54:48 PM.

This paper reports, for the first time, the piezoresistive effect of p-type single crystalline 3C-SiC nanothin films grown by LPCVD at low temperature. Compared to thick SiC films, the gauge factors of the 80 nm and 130 nm films decreased remarkably. This result indicates that the crystal defect at the SiC/Si interface has a significant influence on the piezoresistive effect of ultra-thin film p-type 3C-SiC.

The piezoresistive effect of silicon (Si) has been widely applied in various mechanical sensing devices including pressure sensors, inertial sensors, and strain gauges, thanks to its large gauge factor, miniaturization and electronics integration capability.[1–3] However, the drawbacks of the low energy band gap (1.12 eV) limited the Si material from operating under high temperature conditions.[4] Compared to Si, silicon carbide (SiC), with its large energy band gap of 2.4–3.2 eV and excellent mechanical properties, is one of the most promising materials for applications in harsh environments.[5,6] The piezoresistive effect of SiC has been intensively studied in various polytypes,[7–12] particularly in the cubic crystal (3C-SiC) which has a large gauge factor of about 30.[13–16] The development of various SiC based pressure sensors which have the capability of operating at 500 °C has demonstrated the high potential of the piezoresistive SiC for MEMS (Micro Electromechanical System) devices used at high temperatures.[16–18]

Recently, the effect of strain on nano-scale semiconductors is of great interest, in consideration of the superior properties of their low dimensional structures. The giant piezoresistance found in Si nanowires[19] and Si nanothin films[20] with a piezoresistive coefficient of -3350×10^{-11} Pa^{-1} and 440×10^{-11} Pa^{-1}, respectively, has been a motivation for research into the piezoresistive effect in nanoscale SiC. The piezoresistance of SiC nanowires with a diameter of 150 nm fabricated by the bottom up process which possesses the piezoresistive coefficients comparable with Si has been reported.[7–9] To the best of our knowledge, to date, there have been no reports on the characterization of the piezoresistive effect in SiC nanothin films with the thickness below 150 nm fabricated by the top down process. Compared to the bottom up method, the top down method takes full advantage of the compatibility with the conventional fabrication process as well as packaging for MEMS devices. Therefore, research on the electromechanical properties of the top down fabricated SiC nanothin film and nanowire is extremely important for the development of low dimensional SiC based MEMS sensors in future.

In this paper, we characterize, for the first time, the piezoresistive effect of p-type single crystalline 3C-SiC nanothin films grown by LPCVD (low pressure chemical vapor deposition). Various 3C-SiC films with thickness ranging from 80 nm to 1 μm have been fabricated to investigate the thickness dependence of the piezoresistive effect in p-type 3C-SiC.

The 3C-SiC was grown on a Si(100) substrate using a hot-wall LPCVD reactor at 1000 °C.[21] The alternating supply epitaxy (ASE) approach was used to achieve single crystalline SiC film deposition with silane (SiH_4) and propylene (C_3H_6) as precursors. Trimethylaluminium [$(CH_3)_3Al$] was employed as a p-type dopant for *in situ* doping. The thickness of the SiC films was controlled by varying the number of growth cycles and measured by using a spectrophotometer Nanospec AFT 210. After the epitaxial growth process, the SiC piezoresistor was fabricated on a Si substrate by a conventional photolithography process to form SiC/Si strips. Since the 3C-SiC films have different thicknesses, the SiC resistors reflect different colors when observed under an optical microscope, as shown in Fig. 1(a)–(e). The concept of the SiC/Si beam is shown in Fig. 1(f), by which the SiC resistor was patterned into a U-shaped structure to characterize the piezoresistive effect. Additionally, two aluminum contact pads were fabricated at each end of the SiC resistor, so that the four-terminal resistance measurement could be performed to eliminate the contact resistance.

[a]Queensland Micro-Nanotechnology Centre, Griffith University, Queensland, Australia. E-mail: hoangphuong.phan@griffithuni.edu.au

[b]School of Engineering, Griffith University, Queensland, Australia

† Electronic supplementary information (ESI) available: Electrical characterization and the deduction of the total gauge factor of the 3C-SiC resistors. See DOI: 10.1039/c4tc01054j

This journal is © The Royal Society of Chemistry 2014

Published on 18 July 2014. Downloaded by Griffith University on 3/14/2021 10:54:48 PM.

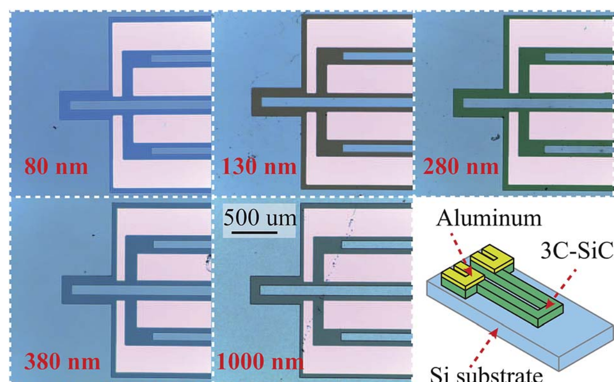

Fig. 1 From (a) to (e): photographs of SiC resistors on a Si substrate. Different thicknesses reflect different colors. (f) The concept of the SiC/Si beam designed for the bending experiment.

The hot probe technique was carried out to characterize the doping type and the carrier concentration of the 3C-SiC films. The positive voltage in the hot probe indicates that the SiC films were p-type semiconductors. Table 1 shows the results of the hot probe measurement in which the carrier concentrations of the grown p-type SiC films were in the same range of approximately 1.4–10 $\times$ 10^{18} cm^{-3}, indicating that all 3C-SiC films are normally doped semiconductors in which the dopant was aluminum. As the SiC (carrier concentration $N \simeq 10^{18}$ cm^{-3}) was grown on a Si substrate (carrier concentration $N \simeq 10^{14}$ cm^{-3}), the issue of current leakage through the SiC/Si junction was investigated to ensure that the Si substrate did not contribute to the measured gauge factor. In all 3C-SiC resistors, the I–V curves show good linearity indicating the ohmic contact, and the ratio of the current leakage to the current through the SiC resistor was below 0.5% (ESI†).

In our previous study on the orientation dependence of the piezoresistive effect in p-type 3C-SiC, we found that the piezoresistive effect is dominated by the shear piezoresistive coefficient π_{44}, and the [110] orientation possesses the largest gauge factor.[14] Therefore, in this study, we focus on characterizing the longitudinal gauge factor of the [110] direction of the p-type single crystalline 3C-SiC films. The piezoresistive effect of 3C-SiC was measured by the bending method in which one end of the SiC/Si beam was fixed by a metal clamp, and the other end was pushed by a load (Fig. 2(a)). The strain of the SiC resistor was obtained from the Finite Element Method (FEM) and conventional theoretical calculation. The simulation results

Table 1 Hot probe measurement on different thickness films[a]

Film thickness (nm)	V_{oc} [mV]	I_{sc} [nA]	Carrier concentration N [cm^{-3}]
1000	9.8	−1940	1.4–6.2 $\times$ 10^{18}
380	8.5	−1057	2.5–10 $\times$ 10^{18}
280	9.6	−670	1.5–6.8 $\times$ 10^{18}
130	9.4	−480	1.5–7.0 $\times$ 10^{18}
80	9.9	−75	1.3–6.0 $\times$ 10^{18}

[a] V_{oc}: the open circuit voltage; I_{sc}: the short circuit current.[22]

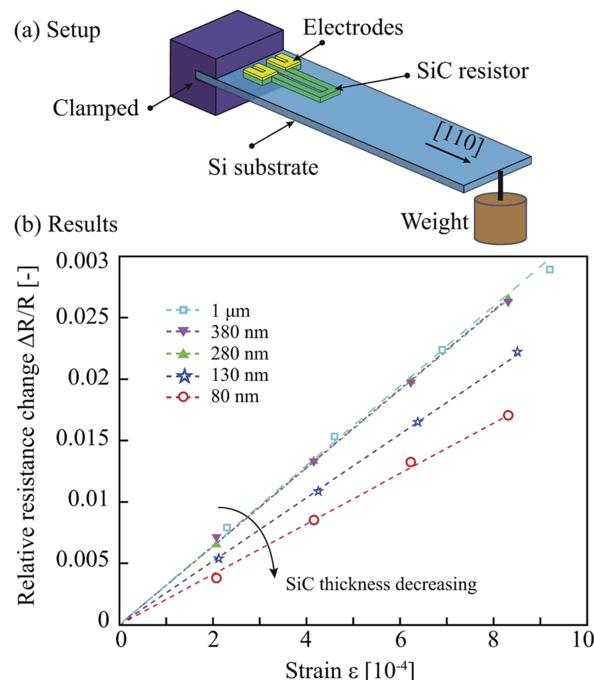

Fig. 2 (a) The setup of the bending experiment. (b) The relationship between the relative resistance change of 3C-SiC resistors and applied strain. The relative resistance changes of the 1 μm, 380 nm and 280 nm films are almost the same, while it decreases considerably in the 130 nm and 80 nm thin films.

(Comsol Multiphysics) show that the strain distribution in the SiC resistor is relatively uniform. It is approximately the same as the strain of the top surface of the Si substrate (ESI†). Fig. 2(b) shows the linear relationship between the relative resistance change of the p-type 3C-SiC and the applied tensile strain varied from 0 ppm to approximately 1000 ppm. By using our calculation method,[13,14] we obtained the longitudinal gauge factor in the [110] orientation of the 80 nm, 130 nm, 280 nm, 380 nm and 1 μm films to be 20.5, 26.1, 30.3, 30.4 and 31.1, respectively. It can be seen that the gauge factor of the p-type single crystalline 3C-SiC is relatively consistent in SiC films with the thickness above 280 nm. Nevertheless, in the thinner films with the thickness of 80 nm and 130 nm, the gauge factor decreased considerably (about 65.9% and 83.9% compared to the 1 μm film). It should be noticed that in the film with thickness above 80 nm, the effect of quantum confinement is negligible.[19] Additionally, since the SiC was epitaxially grown on a Si substrate which has a different lattice size of 20% and a thermal expansion mismatch of 25%, the crystal defect at the SiC/Si interface is a serious concern in the epitaxial SiC. The crystal defects were reported to have a significant influence on the electrical/mechanical properties of the single crystalline SiC.[15,23] In our previous work, the crystalline quality of the 3C-SiC films with different thicknesses was characterized by measuring the FWHM (full width at half maximum) of the rocking curve scan.[21] The continuous reduction of the FWHM confirmed that the crystal quality is improved with an increase in film thickness. Additionally, the mobility factor obtained from the hot probe measurement showed that the carrier mobility of the 80 nm film

Published on 18 July 2014. Downloaded by Griffith University on 3/14/2021 10:54:48 PM.

(approximately ~7.5 $cm^2 V^{-1} s^{-1}$) was smaller than that of the 280 nm film (approximately ~15 $cm^2 V^{-1} s^{-1}$). This result indicated that the crystal defect reduced the conductivity of the epitaxy 3C-SiC thin films due to defect scattering. Therefore, the crystal defect should be taken into account to explain the reduction of the gauge factor in the 3C-SiC thin films.

The quality of the SiC films was investigated by the TEM (Transmission Electron Microscopy) image, which shows that the crystal defect appeared in the single crystalline 3C-SiC (Fig. 3(a)). A high density of defects was observed at the SiC/Si interface (dominantly the stacking faults in the [111] orientation), particularly at the bottom 60 nm from the SiC/Si interface. It is also clear in the TEM image that the quality of the films improved with increasing the distance from the interface, which is in solid agreement with other work.[15,21] To simplify our model, we assume that:

(i) The SiC film consists of two layers: the low density defect layer at the top, and the high density defect layer at the bottom (Fig. 3(a)). As the 3C-SiC films in this study were grown by the same LPCVD process, the high defect density layer in these films is expected to have the same thickness. The total conductance of the SiC films (G_t) is

$$G_t = G_{ld} + G_{hd} \quad (1)$$

where G_{ld} and G_{hd} are the conductance of the low density defect layer and high density defect layer, respectively.

(ii) The ratio of the conductance of the high density defect layer to the total conductance of the SiC film is a monotonically decreasing function of the films thickness ($f(t)$ decreases when t increases, ESI†).

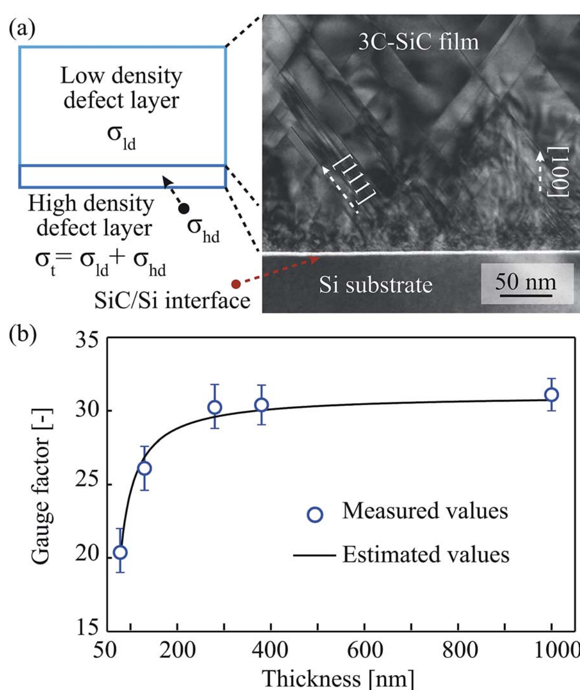

Fig. 3 TEM image of a 3C-SiC film and the comparison between estimated values and the experimental results of the gauge factor.

$$G_{hd}/G_t = f(t_{SiC}) \quad (2)$$

where t_{SiC} is the thickness of SiC films.

When a strain is applied on the SiC film, the conductance of the high density defect layer and low density defect layer changes to $G_{hd} + \Delta G_{hd}$ and $G_{ld} + \Delta G_{ld}$, respectively. The gauge factor of SiC is defined as

$$\mathrm{GF} = \frac{\Delta R}{R} \times \frac{1}{\varepsilon} \approx -\frac{\Delta G_t}{G_t} \times \frac{1}{\varepsilon} \quad (3)$$

Thus, the measured gauge factor is (ESI†)

$$\begin{aligned}\mathrm{GF} &= -\frac{\Delta G_{ld} + \Delta G_{hd}}{G_t} \times \frac{1}{\varepsilon} = \frac{G_{hd}}{G_t}\mathrm{GF}_{hd} + \left(1 - \frac{G_{hd}}{G_t}\right)\mathrm{GF}_{ld} \\ &= f(t_{SiC})\mathrm{GF}_{hd} + (1 - f(t_{SiC}))\mathrm{GF}_{ld}\end{aligned} \quad (4)$$

where GF_{ld} and GF_{hd} are the gauge factors of the low density defect layer and high density defect layer, respectively. For a thick SiC film, the ratio of G_{hd}/G_t is sufficiently small (see eqn (2)). Therefore, the measured gauge factor can be approximately equal to the gauge factor of the low density defect layer GF_{ld}. Using eqn (4), we estimated the thickness dependence of the piezoresistive effect in p-type 3C-SiC, as shown in Fig. 3(b). The experiment results matched well with the calculation based on the proposed model.

In summary, the piezoresistive effect of p-type single crystalline 3C-SiC ultra-thin films grown on a p-type Si (100) substrate by the LPCVD process has been characterized. A giant piezoresistive effect was not observed in nanothin films with a thickness of 80 nm or thicker. The consistency of the gauge factor of the SiC layer with a thickness above 280 nm, and the large drop of the gauge factor in the 80 nm and 130 nm films imply that the crystal defect has a significant influence on the piezoresistive effect of the p-type single crystalline 3C-SiC nanothin film with thickness below 150 nm, while this influence is negligible in sufficiently thick films.

Acknowledgements

This work was performed in part at the Queensland node of the Australian National Fabrication Facility, a company established under the National Collaborative Research Infrastructure Strategy to provide nano and micro-fabrication facilities for Australia's researchers. This work has been partially supported by the Griffith University's New Researcher Grants.

References

1 D. V. Dao, T. Toriyama, J. Wells and S. Sugiyama, *Sens. Mater.*, 2003, **15**(3), 113.
2 D. V. Dao, K. Nakamura, T. T. Bui and S. Sugiyama, *Adv. Nat. Sci.: Nanosci. Nanotechnol.*, 2010, **1**(1), 013001.
3 A. A. Barlian, W. T. Park, J. R. Mallon Jr, A. J. Rastegar and B. L. Pruitt, *Proc. IEEE*, 2009, **97**(3), 513.
4 P. M. Sarro, *Sens. Actuators, A*, 2000, **82**(1–3), 210.
5 Y. Chen, X. Zhang, Q. Zhao, L. He, C. Huang and Z. Xie, *Chem. Commun.*, 2011, **47**, 6398.

This journal is © The Royal Society of Chemistry 2014

6 M. Mehregany, C. A. Zorman, N. Rajan and C. H. Wu, *Proc. IEEE*, 1998, **86**(8), 1594.
7 J. Bi, G. Wei, L. Wang, F. Gao, J. Zheng, B. Tang and W. Yang, *J. Mater. Chem. C*, 2013, **1**, 4514.
8 F. Gao, J. Zheng, M. Wang, G. Wei and W. Yang, *Chem. Commun.*, 2011, **47**, 11993.
9 R. Shao, K. Zheng, Y. Zhang, Y. Li, Z. Zhang and X. Han, *Appl. Phys. Lett.*, 2012, **101**, 233109.
10 T. Akiyama, D. Briand and N. F. Rooij, *J. Micromech. Microeng.*, 2012, **22**, 085034.
11 M. A. Fraga, H. Furlan, R. S. Pessoa, *et al.*, *Microsyst. Technol.*, 2012, **18**, 1027.
12 R. S. Okojie, A. A. Ned, A. D. Kurtz and W. N. Carr, *IEEE Trans. Electron Devices*, 1998, **45**(4), 785.
13 H. P. Phan, P. Tanner, D. V. Dao, N. T. Nguyen, L. Wang, Y. Zhu and S. Dimitrijev, *IEEE Electron Device Lett.*, 2014, **35**(3), 399.
14 H. P. Phan, D. V. Dao, P. Tanner, N. T. Nguyen, L. Wang, Y. Zhu and S. Dimitrijev, *Appl. Phys. Lett.*, 2014, **104**, 111905.
15 M. Eickhoff, M. Moller, G. Kroetz and M. Stutzmann, *J. Appl. Phys.*, 2004, **96**, 2872–2879.
16 S. J. Shor, D. Goldstein and A. D. Kurtz, *IEEE Trans. Electron Devices*, 1993, **40**(6), 1093.
17 C. H. Wu, C. A. Zorman and M. Mehregany, *IEEE Sens. J.*, 2006, **6**(2), 316.
18 R. Ziermann, J. V. Berg, E. Obermeier, F. Wischmeyer, E. Niemann, H. Moller, M. Eickhoff and G. Kroetz, *Mater. Sci. Eng., B*, 1999, **61–62**, 576.
19 R. He and P. Yang, *Nat. Nanotechnol.*, 2006, **1**, 42.
20 Y. Yang and X. Li, *Nanotechnology*, 2011, **22**, 015501.
21 L. Wang, S. Dimitrijev, J. Han, A. Iacopi, L. Hold, P. Tanner and H. B. Harrison, *Thin Solid Films*, 2011, **519**, 6443.
22 P. Tanner, L. Wang, S. Dimitrijev, J. Han, A. Iacopi, L. Hold and G. Walker, *Sci. Adv. Mater.*, 2014, **6**, 1542.
23 X. Song, J. F. Michaud, F. Cayrel, M. Zielinski, M. Portail, T. Chassagne, E. Collard and D. Alquier, *Appl. Phys. Lett.*, 2010, **96**, 142104.

Published on 18 July 2014. Downloaded by Griffith University on 3/14/2021 10:54:48 PM.